

Normalization of the Matter Power Spectrum via Higher-Order Angular Correlations of Luminous Red Galaxies

Ashley J. Ross¹, Robert J. Brunner^{1,2}, Adam D. Myers¹

aross2@uiuc.edu

ABSTRACT

We present a novel technique to measure σ_8 , by measuring the dependence of the second-order bias of a density field on σ_8 using two separate techniques. Each technique employs area-averaged angular correlation functions ($\bar{\omega}_N$), one relying on the shape of $\bar{\omega}_2$, the other relying on the amplitude of s_3 ($s_3 = \bar{\omega}_3/\bar{\omega}_2^2$). We confirm the validity of the method by testing it on a mock catalog drawn from Millennium Simulation data and finding $\sigma_8^{measured} - \sigma_8^{true} = -0.002 \pm 0.062$. We create a catalog of photometrically selected LRGs from SDSS DR5 and separate it into three distinct data sets by photometric redshift, with median redshifts of 0.47, 0.53, and 0.61. Measurements of c_2 , and σ_8 are made for each data set, assuming flat geometry and WMAP3 best-fit priors on Ω_m , h , and Γ . We find, with increasing redshift, $c_2 = 0.09 \pm 0.04$, 0.09 ± 0.05 , and 0.09 ± 0.03 and $\sigma_8 = 0.78 \pm 0.08$, 0.80 ± 0.09 , and 0.80 ± 0.09 . We combine these three consistent σ_8 measurements to produce the result $\sigma_8 = 0.79 \pm 0.05$. Allowing the parameters Ω_m , h , and Γ to vary within their WMAP3 1σ error, we find that the best-fit σ_8 does not change by more than 8% and we are thus confident our measurement is accurate to within 10%. We anticipate that future surveys, such as Pan-STARRS, DES, and LSST, will be able to employ this method to measure σ_8 to great precision, and will serve as an important check, complementary, on the values determined via more established methods.

Subject headings: Cosmology: Observations, Large Scale Structure

¹Department of Astronomy, University of Illinois at Urbana-Champaign, Urbana, IL 61801

²National Center for Supercomputing Applications, Champaign, IL 61820

1. Introduction

The normalization of the matter power spectrum is parameterized as the *rms* mass fluctuation within a top-hat radius of $8h^{-1}\text{Mpc}$ and denoted σ_8 . Measuring the amplitudes of the matter power spectrum, and thus σ_8 , is complicated by the fact that most of the matter in the Universe is dark and that we must therefore rely on “tracers” of the matter — in most cases galaxies. There is no guarantee, of course, that galaxies will cluster in the same manner as dark matter. The relationship between the clustering of galaxies and dark matter is known as the “bias” (see, e.g., Kaiser 1984). The bias essentially shifts the amplitudes of the galaxy power spectrum relative to the matter power spectrum and there is thus a strong degeneracy between the bias and σ_8 . Therefore, precisely determining σ_8 is important, as until this is accomplished, the full form of the relationship between the clustering of dark matter and the clustering of galaxies will remain ambiguous.

Measurements of σ_8 made using cluster counting techniques find mixed results. Using the X-ray temperature and luminosity functions and fully marginalizing over the cluster scaling relation, Pierpaoli et al. (2003) found $\sigma_8 = 0.77^{+0.05}_{-0.04}$, while Henry (2004) found $\sigma_8 = 0.66 \pm 0.16$. Using a self-calibration technique and the red-sequence to optically identify clusters in the red-sequence cluster survey, Gladders et al. (2007) found $\sigma_8 = 0.67^{+0.18}_{-0.13}$, while Rozo et al. (2007) found $\sigma_8 = 0.92 \pm 0.10$ using the SDSS maxBCG (Koester et al. 2007) catalog. Clearly, there is large variation in the measurements of σ_8 determined via cluster abundances.

Measurements made using data from the Wilkinson Microwave Anisotropy Probe (WMAP) place some of the best constraints on the value of σ_8 , yet still allow a wide range of values. The first year WMAP (WMAP1) results found $\sigma_8 = 0.92 \pm 0.10$ (Spergel et al. 2003), while the third year (WMAP3) results determined $0.744^{+0.05}_{-0.06}$ (Spergel et al. 2007). The best-fit WMAP3 results vary significantly depending on the adopted constraints and priors. In the currently accepted cosmological paradigm, inflation is a key ingredient. When WMAP3 is constrained by a variety of inflationary models, the best-fit σ_8 are found to be as low as 0.702 ± 0.062 (Spergel et al. 2007). If one instead combines the WMAP3 results with the Sloan Digital Sky Survey (SDSS) galaxy power spectrum (Tegmark et al. 2004), $\sigma_8 = 0.772^{+0.041}_{-0.042}$. Considering the importance of inflation to our understanding of the Universe, the constraints placed by WMAP3 are quite loose. Analysis of the WMAP 5 year data (WMAP5; made public during the revision process of this work) yielded a best-fit 5-year mean value of 0.796 ± 0.036 (Komatsu et al. 2008). Despite the precision of this value, if one considers the high and low values measured by WMAP1 and WMAP3 and the range in values determined via cluster counting techniques, the true value of σ_8 remains unclear.

In this paper, we present a novel technique to measure σ_8 . Our technique relies on the

fact that the bias relationship may be non-linear and if the bias is non-linear, then both the amplitude and the shape of the correlation function (the Fourier transform of the power spectrum) are affected. As the value of σ_8 affects only the amplitude of the correlation function measurement, the non-linear bias is not degenerate with σ_8 . Therefore, different techniques for measuring the extent of the non-linear bias can constrain not only the non-linear bias, but σ_8 as well.

The bias relationship can be expressed as a Taylor expansion, with the parameters b_1 and b_2 representing the first- and second-order contributions (and b_2 thus being a measure of the non-linearity; see, e.g., Gaztanaga 1992). In general, it is convenient to express the second-order contribution as $c_2 = b_2/b_1$. The average overdensity increases as the scale becomes smaller, therefore the effect of c_2 increases on smaller scales. If c_2 is positive, the correlation function will be increasingly amplified towards smaller scales. Thus, transitioning between the non-linear and linear regime ($\sim 10 h^{-1}\text{Mpc}$, the “weakly non-linear regime”) the bias relationship changes such that b_2 transitions from having little effect on the measurement to having an important effect. Therefore, it is ideal to test c_2 using correlation functions at scales on either side of the weakly non-linear regime, as the effects of b_1 and b_2 can be decoupled by considering both small and large scales.

Photometrically selected luminous red galaxies (LRGs) from the SDSS DR5 imaging data are ideal for measuring correlation functions in the weakly non-linear regime. The median redshift of SDSS LRGs is ~ 0.52 , meaning that $10 h^{-1}\text{Mpc}$ is equivalent to about 0.4 degrees—a scale at which angular galaxy correlation functions in SDSS can be calculated quite precisely. Thus, by studying the shape of the 2-point area-averaged correlation function ($\bar{\omega}_2$) of LRGs around these scales, one can measure c_2 quite precisely. This measurement is dependent on σ_8 and therefore one can determine the relationship between the non-linear bias of LRGs and σ_8 . A separate relationship between the non-linear bias and σ_8 can be found by utilizing the shape of the hierarchical amplitude $s_3 = \bar{\omega}_3/(\bar{\omega}_2)^2$ (see, e.g., Ross et al. 2007; R07 from hereon). These two relationships are nearly orthogonal, thereby allowing unambiguous determinations of b_1 , c_2 , and σ_8 .

This is not the first study of the clustering of photometrically selected LRGs. Padmanabhan et al. (2007) and Blake et al. (2007) selected LRGs from SDSS imaging data and studied their clustering. These efforts measured the two-point correlation function and power-spectrum, respectively, at different redshifts to place tight constraints on the matter and baryon densities of the universe (but not σ_8). Nor is this the first study to measure the higher-order clustering of LRGs, as Kulkarni et al. (2007) measured the redshift space three-point correlation function of spectroscopically selected LRGs.

Our work, however, has three major distinctions from these previous studies: (1) our

data is drawn from the contiguous area of SDSS DR5, significantly improving our ability to calculate higher-order statistics at large scales, (2) we measure higher-order statistics using photometrically selected LRGs and thus the median redshift is higher than for any previous sample used to study the higher-order clustering of LRGs, and (3) we focus on determining the value of σ_8 . We will outline our methods for determining the two separate relationships between σ_8 and c_2 in §2. In §3, we will describe the creation of a photometric redshift catalog of LRGs drawn from the SDSS DR5 imaging data, which follows the prescriptions of Collister et al. (2007). In §4, we will present precise measurements of the second- and third-order angular area-averaged correlation functions of LRGs. We will display our measurements of the first- and second-order bias parameters of LRGs, and we will show that these bias parameters have a strong dependence on σ_8 . We combine these measurements to present a precise measurement of σ_8 .

Unless otherwise noted, we assume a flat cosmology with parameters equal to the WMAP3 alone best-fit values $(\Omega_m, h, \Gamma) = (0.238, 0.73, 0.135)$, where Γ is the shape parameter, and essentially parameterizes Ω_b assuming fixed Ω_m and h (see, e.g., Equations 30 and 31 of Eisenstein & Hu 1998).

2. Methods

2.1. Angular Correlation Functions

We estimate N-point area-averaged angular correlation functions, $\bar{\omega}_N(\theta)$, using a counts-in-cells technique identical to that used in R07. This involves calculating the statistical moments of the over-densities contained in equal-area cells. We create the cells using a modified version of the *SDSSpix* pixelization scheme originally developed by Tegmark, Xu, and Scranton¹. The over-density for cell i is defined as

$$\delta_i = \frac{\bar{n} - n_i}{\bar{n}} \quad (1)$$

where \bar{n} is the average number of galaxies in a cell and n_i is the number of galaxies in cell i . The remaining details and equations required to determine $\bar{\omega}_N(\theta)$ are found in Ross et al. (2006). The hierarchical amplitudes are defined as

$$s_N = \frac{\bar{\omega}_N}{\bar{\omega}_2^{N-1}} \quad (2)$$

¹<http://lahmu.phyast.pitt.edu/~scranton/SDSSPix/>

2.2. Bias and σ_8

In order to determine the relationship between the bias parameter c_2 and σ_8 , measurements of $\bar{\omega}_2$ and s_3 are compared to theoretical models constructed via matter power spectra. In each case, the $z = 0$ value of σ_8 is input to the model, allowing $c_2(\sigma_8)$ to be calculated.

Model $\bar{\omega}_2$ are produced using power spectra calculated using the Smith et al. (2003) fitting formulae, as described in R07 §6. By using a modified version of Limber’s equation (Limber 1954), one can use the redshift distribution of our LRG catalog to invert the $P(k)$ and obtain $\bar{\omega}_2(\theta)$:

$$\bar{\omega}_2(\theta) = \frac{H_0\pi}{c} \int \int \left(\frac{dn}{dz} \right)^2 \sqrt{\Omega_m(1+z)^3 + \Omega_\Lambda} P(k, z) W_{2D}^2[\chi(z)\theta k] dz dk \quad (3)$$

where $W_{2D} = 2 \frac{J_1(x)}{x}$ is the top-hat two-dimensional window function, $\chi(z)$ is the comoving distance to redshift z , $P(k, z)$ is the matter power spectra, k is the spectral index, and J_1 is the first-order Bessel function of the first kind, and this equation requires $\Omega_{total} = 1$ (see, e.g., Bernardeau et al. 2002). This equation is then integrated using the assumed cosmology and the desired value of σ_8 .

Both methods employed to measure c_2 are dependent on the product of b_1 and σ_8 . In order to account for this, we determine the first-order bias using the $\bar{\omega}_2$ measurement and the model $\bar{\omega}_2$ at $\sigma_8 = 0.8$ and denote it $b_{1,0.8}$. This is calculated for scales where linear theory is a good approximation ($> 10h^{-1}$ Mpc). Therefore, a valid expression for the first-order bias is given by $b_{1,LRG} = (0.8/\sigma_8) b_{1,0.8}$.

The second-order bias can be determined by manipulating the overdensities in each cell used in the calculation of $\bar{\omega}_2$. The overdensity of LRGs can be related to the overdensity of dark matter and bias terms via a Taylor expansion (to second order)

$$\delta_{LRG} = b_1\delta_{DM} + 0.5b_2\delta_{DM}^2 \quad (4)$$

In order to apply a second order bias term to the LRG correlation measurement, one must solve Equation 4 for δ_{DM} , which, to second order, is

$$\delta_{DM} = \delta_{LRG}/b_1 - 2b_2\delta_{LRG}^2/b_1^3 \quad (5)$$

Thus, in order to determine the first and second order bias of the LRGs, we use Equation 5 to apply a b_1 and a b_2 to each overdensity used in the measurement of $\bar{\omega}_2$ and match these altered measurements to the model $\bar{\omega}_2$. To find the best fit b_2 for a given σ_8 , one must simply calculate $\bar{\omega}_2$ for a sampling of b_2 values, calculate the χ^2 for each, and minimize χ^2

via iteration (fully accounting for covariance as noted in §4). This must then be repeated for all of the σ_8 values one wishes to test (which requires determining the model $\bar{\omega}_2$ for each σ_8). This process requires the correlation functions to be calculated thousands of times, but is highly parallel. In practice, we determine the χ^2 values for selected σ_8/b_2 values on a grid of initial spacing 0.02 in σ_8 and 0.005 in b_2 . This grid is then refined in areas of rapidly changing χ^2 . The χ^2 value for any σ_8/b_2 pair is then found by using a two dimensional spline fit to the grid. This method will hereon be referred to as the *shape* method.

The other method we employ is detailed in R07, and takes advantage of the relationship (Fry & Gaztanaga 1993)

$$s_3 = b_1^{-1}(s_{3,DM} + 3c_2) \quad (6)$$

where s_3 is the measured amplitude and $s_{3,DM}$ is the theoretical amplitude. The $s_{3,DM}$ are determined at scales greater than $8 h^{-1}\text{Mpc}$. This is accomplished by calculating $\bar{\omega}_3$ via the integration of linear power spectra and redshift distributions given by Bernardeau (1995),

$$\bar{\omega}_{3,DM} = 6 \left(\frac{H_0\pi}{c}\right)^2 \int \left(\frac{dn}{dz}\right)^3 [\Omega_m(1+z)^3 + \Omega_\Lambda] dz \times \left\{ \frac{6}{7} \left(\int kP(k)W_{2D}^2[D\theta k]dk\right)^2 + \int kP(k) (W_{2D}^2[D\theta k]) dk \int k^2 D\theta P(k)W_{2D}[D\theta k]W'_{2D}[D\theta k]dk \right\} \quad (7)$$

where D is the comoving distance to the median redshift. We calculate $\bar{\omega}_2$ using Equation 3 and linear power spectra and then use $s_3 = \bar{\omega}_3/\bar{\omega}_2^2$. By altering σ_8 and using the relationship described in §7.1, Equation 14, of R07, we can determine the 1σ allowed region of c_2/σ_8 . We will refer to this approach as the *R07* method.

2.3. Testing via Mock Catalogs

To test our new method, we took galaxies with $M_r < -23$ from the Blaizot all-sky mock catalog created using the methods described in Blaizot et al. (2005) and Millennium Simulation data (Springel et al. 2005). In order to select red galaxies we constrained the absolute magnitudes of our mock catalog to have $B - R > 1.4$, as we discovered that the color of the simulated galaxies was bimodal about this value. This yielded a sample of nearly 300,000 simulated LRGs. These simulated LRGs had a median redshift of 0.2; this is significantly smaller than the LRGs to be used in our measurements, but nonetheless quite sufficient to test our measurement techniques.

Using our mock catalog, $\bar{\omega}_N$ and s_N were calculated using the methods described in §2.1. In order to determine the bias of the simulated LRGs, we employed the methods described in §2, to calculate model $\bar{\omega}_N$ and s_N . This was done using $\sigma_8 = 0.8$ and the assumed

cosmology of the Millennium Simulation (relevant parameters being Ω_m , h , $\Gamma = 0.25, 0.73, 0.14$; Springel et al. 2005). This allowed us to find $b_{1,0.8} = 2.04 \pm 0.02$, fit at scales $> 8.2 h^{-1}\text{Mpc}$ ($> 0.8^\circ$). With this value in hand, we could then use the *shape* method to find the χ^2 values in the b_2/σ_8 parameter space. This allowed us to find the best-fit c_2 value as a function of σ_8 . These 1σ bounds, which represent $\Delta\chi^2 = 1$ from the minimum at that σ_8 , are displayed on Figure 1 by solid black lines. For $\sigma_8 = 0.8$, we found $c_2 = 0.186 \pm 0.026$.

Using the *R07* method and setting $\sigma_8 = 0.8$, we found $c_2 = 0.41 \pm 0.09$. The large disagreement with the value of c_2 determined by the *shape* and *R07* methods is expected for $\sigma_8 = 0.8$, as the two methods should agree only for the σ_8 used to create the mock catalog (0.9). To find where the methods agreed, we calculated χ^2 for the entire c_2/σ_8 parameter space using the *R07* method. The resulting 1σ allowed region, which represent $\Delta\chi^2 = 1$, is bounded by the dashed black lines in Figure 1. Combining the χ^2 distributions of the two methods produced the 1σ ($\Delta\chi^2 = 2.3$ from the overall minimum) region displayed in red in Figure 1. From these measurements, we determine $\sigma_8 = 0.898 \pm 0.062$ and $c_2 = 0.146 \pm 0.037$. This measured σ_8 is entirely consistent with the input $\sigma_8 = 0.9$ of the Millennium Simulation. This confirms that our method can indeed be used to measure the value of σ_8 both precisely and accurately.

3. Data

We take data from the fifth data release (DR5) of the Sloan Digital Sky Survey. To create a catalog of LRGs with photometric redshifts we applied the techniques described by Collister et al. (2007) (abbreviated C07 from here on) applied to objects in the DR5 *PhotoPrimary* view. Employing the color and magnitude cuts described by C07 produces a sample of just over 1.7 million objects. As in C07, we found photometric redshifts by using the *annz* software (Firth et al. 2003) with the Two-Degree Field SDSS LRG and QSO (2SLAQ) spectroscopic LRG catalog (Cannon et al. 2006), with stars removed, as training data. In order to separate stars, we again used the *annz* software, and trained it on the 2SLAQ LRG target catalog. In this case, we included the targeted objects determined to be stars and gave them a classification value of 0, while galaxies were given a classification value of 1. This same method was employed by C07 to eliminate stars from their catalog.

Our final catalog comprises only objects with classification values greater than 0.8. Based on the training data, cutting on this value should reduce stellar contamination to less than 2% while keeping 99.9% of the LRGs. This results in a catalog of 1,662,390 LRGs with a median photometric redshift of 0.52. Our redshift distribution is nearly identical to the distribution found by C07. These LRGs are then processed through the same imag-

ing/reddening/seeing masks as in R07, leaving 1,168,702 objects. We split these LRGs into three distinct photometric redshift ranges with similar numbers of objects, $0.4 < z < 0.5$ (444,175 LRGs), $0.5 < z < 0.57$ (398,250 LRGs), and $0.57 < z < 0.7$ (326,277 LRGs). These data sets will be referred to as $Z_{0.47}$, $Z_{0.53}$, and $Z_{0.61}$, with median redshifts of 0.47, 0.53, and 0.61, respectively. This gives us three distinct data sets that allow us to test the consistency of our measurements and that can be combined to increase the precision of our final σ_8 measurement.

4. Measurements

We calculate the area-averaged angular correlation functions ($\bar{\omega}_N$) and hierarchical amplitudes (s_N) for photometrically classified SDSS DR5 LRGs using the methods described in §2.1. For every measurement, errors and covariance matrices are calculated using a jackknife method (e.g., Scranton et al. 2002), with inverse-variance weighting for both errors (e.g., Myers et al. 2005, 2006) and covariance (e.g., Myers et al. 2007), identical to the one described in §3.4 of R07. This allows us to minimize χ^2 , fully accounting for covariance via

$$\chi^2 = \sum_{i,j} [\bar{\omega}(\theta_i) - \bar{\omega}_m(\theta_i)] C_{i,j}^{-1} [\bar{\omega}(\theta_j) - \bar{\omega}_m(\theta_j)] \quad (8)$$

where C is the covariance matrix, and i and j refer to the i^{th} and j^{th} jackknife subsample.

Focusing first on $Z_{0.53}$, we fit $\bar{\omega}_2$ for measurements made between 0.4° and 1.6° ($10.2 h^{-1}\text{Mpc}$ and $40.2 h^{-1}\text{Mpc}$). We determine $b_{1,0.8} = 1.63 \pm 0.02$. The $\bar{\omega}_2$ is well fit by a single bias parameter in this range, as the $\chi^2 = 1.7$, $P(< \chi^2) = 0.89$. Thus, we measure $b_{1,LRG} = 0.8/\sigma_8 \times (1.63 \pm 0.02)$. The $\bar{\omega}_2$ measurement is presented in Figure 2, divided by 1.63^2 (accounting for $b_{1,0.8}$) along with the model $\bar{\omega}_2$ at $\sigma_8 = 0.8$. At scales less than 0.3° , the measurement grows larger than the model, indicative of positive second-order bias. The measurement also grows larger at scales greater than $\sim 2^\circ$ ($50.2 h^{-1}\text{Mpc}$), but at these scales the errors begin to grow larger and systematics due to reddening and projection effects also increase. Based on the results of Simon (2007), our theoretical curve, which employs a modified version of Limber’s Equation, should not be accurate to better than 10% at scales greater than $\sim 2^\circ$ for any of the redshift ranges we use. Our measurement at 2° differs from the model by 8.5%, thus the disagreement is no greater than would be predicted by Simon (2007). We thus fit no measurements to scales greater than 1.6° .

Altering the $\bar{\omega}_2$ measurement using the *shape* method, and fitting the measurements at scales between 0.1° and 0.7° (equivalent to ~ 2.5 to $17.6 h^{-1}\text{Mpc}$, there are 8 measurements in this range and thus 7 degrees of freedom), we measure $b_2 = 0.15 \pm 0.05$ for $\sigma_8 = 0.8$. The

fit is acceptable, as $\chi^2 = 0.60$, $P(< \chi^2) = 0.999$. Attempting to fit the data with a single bias parameter model, we find $\chi^2 = 12.18$, $P(< \chi^2) = 0.09$. For other redshift ranges, we find similar results. Again for $\sigma_8 = 0.8$, we measure $b_{2,Z_{0.47}} = 0.150 \pm 0.040$ ($\chi^2 = 0.49$, $P(< \chi^2) = 0.999$). A single bias parameter model is rejected at 87%. Finally, we find $b_{2,Z_{0.61}} = 0.165 \pm 0.025$ ($\chi^2 = 1.91$, $P(< \chi^2) = 0.96$). A single bias parameter is rejected at $> 99\%$ for this redshift range. Based on the marginal rejections of a single-parameter model, a two-parameter model is needed to fit the measurements for each redshift range. For the two lower redshift ranges, the minimum χ^2 values are quite small, implying that perhaps our error bars are overestimated for these redshift ranges, further implying our quoted errors on b_2 are overestimated.

In the bottom right panel of Figure 3, the $\bar{\omega}_2$ measurement corrected for $b_1 = 1.63$ and $b_2 = 0.15$ is displayed along with a theoretical $\bar{\omega}_2$ for $\sigma_8 = 0.8$. The model curve clearly fits the data. The other panels display the measured s_3 (black triangles) for $Z_{0.47}$, $Z_{0.53}$, and $Z_{0.61}$ (left to right, top to bottom) corrected for the best-fit b_1 and c_2 in accordance with Equation 6. Each panel also includes a solid line displaying the model s_3 . The $Z_{0.53}$ measurement appears to be extremely consistent with the model, while the curves defined by the other two measurements do not share the same shape as the model. Despite this fact, the size of the error bars allows the $Z_{0.47}$ and $Z_{0.61}$ measurements to appear consistent with the model.

We use the *R07* method to find c_2 for each data set. For data sets $Z_{0.47}$ and $Z_{0.53}$ we fit between 0.4° and 1.6° (equivalent to $9.0 h^{-1}\text{Mpc}$ and $35.9 h^{-1}\text{Mpc}$ for $Z_{0.47}$ and $10.0 h^{-1}\text{Mpc}$ to $40.2 h^{-1}\text{Mpc}$ for $Z_{0.53}$; there are 7 measurements in this range and thus 6 degrees of freedom). For $Z_{0.61}$, we fit between 0.3° and 1.6° ($8.5 h^{-1}\text{Mpc}$ to $45.6 h^{-1}\text{Mpc}$; again 7 measurements and 6 degrees of freedom). We find that for $\sigma_8 = 0.8$, $c_{2,Z_{0.47}} = 0.08 \pm 0.12$, $c_{2,Z_{0.53}} = 0.07 \pm 0.13$ and $c_{2,Z_{0.61}} = 0.14 \pm 0.16$. For $Z_{0.53}$, $\chi^2 = 0.033$, meaning $P(< \chi^2) = 1.0 - 1.0 \times 10^{-6}$. This is a remarkably small χ^2 value, which one might expect (to a degree) based on how well the measured values appear to match the model, despite the size of the error-bars. This suggests that the error-bars are over-estimated for the s_3 measurements in this redshift range, and thus the error on our c_2 measurements may be overestimated as well. For both the $Z_{0.47}$ and $Z_{0.61}$ ranges, $\chi^2 = 1.5$ with $P(< \chi^2) = 0.96$. These values are quite reasonable, implying that if our errors are being overestimated, it is happening only for the $Z_{0.53}$ range.

Using the *shape* and *R07* methods (see §2.2) the χ^2 values over the entire σ_8/c_2 parameter space are determined for each data sample. The 1σ allowed regions of c_2/σ_8 determined via the *R07* (solid black lines, $\Delta\chi^2 = 1$ from fixed σ_8) and the *shape* (dashed black lines, $\Delta\chi^2 = 1$ from fixed σ_8) methods are plotted in Figure 4 for $Z_{0.53}$. Fortunately, the two methods bound

significantly different regions of parameter space, allowing a precise determination of c_2 and σ_8 . Combining the two measurements produces the 1σ (red triangles, $\Delta\chi^2 = 2.3$ from overall minimum) allowed regions for c_2/σ_8 , and are also displayed in Figure 4. To 1σ precision, we thus find $c_{2,Z_{0.53}} = 0.092 \pm 0.052$ and $\sigma_8 = 0.796 \pm 0.086$. Repeating the process for $Z_{0.47}$, we find $c_{2,Z_{0.47}} = 0.088 \pm 0.041$ and $\sigma_8 = 0.776 \pm 0.080$ and for $Z_{0.61}$, we find $c_{2,Z_{0.61}} = 0.092 \pm 0.033$ and $\sigma_8 = 0.798 \pm 0.094$.

The best fit σ_8 for our three data sets are consistent to 0.275σ . Combining the three measurements, we measure $\sigma_8 = 0.789 \pm 0.050$. Adopting this value in order to determine the first order bias, we find $b_{1,Z_{0.47}} = 1.47 \pm 0.09$, $b_{1,Z_{0.53}} = 1.65 \pm 0.09$, and $b_{1,Z_{0.61}} = 1.80 \pm 0.10$. These values make sense given that the median luminosity of the galaxies increases with redshift since our sample is not volume limited. If we multiply each of the best-fit c_2 measurements by 0.789 divided by the best-fit σ_8 for each respective data set (approximately correct for small changes in σ_8 , based on our *shape* method measurements), we find that $c_{2,Z_{0.47}} = 0.09 \pm 0.04$, $c_{2,Z_{0.53}} = 0.09 \pm 0.05$, and $c_{2,Z_{0.61}} = 0.09 \pm 0.03$ for $\sigma_8 = 0.789$. The fact that there is no significant change in c_2 is moderately surprising and implies differences in the halo occupation distribution (HOD). (If the HOD was not changing as a function of halo mass, c_2 would increase with b_1 , see, e.g., Nishimichi et al. 2007). We will discuss the HOD more in §5.2.

Of interest is the fact that the s_3 measurement for both $Z_{0.47}$ and $Z_{0.61}$ have a local minimum (displayed in the two left panels of Figure 3, but there is no such minimum in the s_3 of $Z_{0.53}$. The minimum is at $\sim 0.6^\circ$, equivalent to $11.4 h^{-1}\text{Mpc}$ for the lower redshift range, while it is at $\sim 0.3^\circ$, equivalent to $8.5 h^{-1}\text{Mpc}$, in the high redshift range. In R07, it was found that early-type galaxies also displayed a minimum in their s_3 measurement at $\sim 10 h^{-1}\text{Mpc}$. As in R07, the errors dominate the LRG measurement (though to a lesser extent), but it appears unlikely that this is a coincidence. The feature is seen at approximately the same physical scale, but at a different angular scale due to the differences in redshift. This rules out any possibility of observational systematics such as seeing or reddening. It is unclear whether the feature may be due to projection effects or complicated halo dynamics that do not affect the middle redshift range.

5. Discussion

We have presented a technique for measuring σ_8 using the 2 and 3-point angular area averaged correlation functions and applied it to photometrically classified LRGs from the SDSS DR5, split into three distinct redshift ranges. Using a method that depends on the shape of $\bar{\omega}_2$ and the technique described in R07, two separate relationships were determined

between σ_8 and $c_{2,LRG}$. These relationships split the degeneracy between bias and σ_8 , allowing an unambiguous determination of the 1st and 2nd order bias and σ_8 . The measured σ_8 in three redshift ranges are consistent and combine for a best-fit $\sigma_8 = 0.789 \pm 0.048$. Our determination of σ_8 is quite precise. It is thus important to investigate the assumptions, implicit and explicit, made when determining our measurements, to compare our measurements to the relevant dark-matter-halo/bias theory, and to investigate how consistent our measurements are with previous results.

5.1. Assumptions

The main assumption that goes into our measurements of c_2 is that the bias can be expressed solely as a function of the overdensity, i.e. it is not a function of both the overdensity and the smoothing scale. If the bias was a strong function of scale, it would invalidate any measurement made using the *shape* method, as a changing b_1 would change the shape of $\bar{\omega}_2$. Similarly, the *R07* technique assumes a constant b_1 and c_2 over the range of scales that are fit. Further, the *R07* measurement is fit at a different range of scales than the *shape* measurement. Bias that is a strong function of scale between $2.5 h^{-1}\text{Mpc}$ and $40 h^{-1}\text{Mpc}$ would completely invalidate any comparison between measurements using the *shape* and the *R07* method, and thus invalidate our σ_8 measurements.

Our assumption that the bias can be expressed solely as a function of the overdensity is validated by the goodness of the fit to our bias-corrected measurements. These measurements demonstrated that, between 0.1° and 1.6° , our $\bar{\omega}_2$ measurement is quite consistent with a two bias parameter model, as all of the model fits using the *shape* method were accepted to better than 96%. Further, in each redshift range, the probability that a single bias parameter fits the data is less than 9%. The simplest model that fits the data between 0.1° and 1.6° is thus that the bias is independent of scale and can be described by two parameters. Therefore, we believe our measurement techniques to be valid and that our comparison of those techniques is valid as well.

The error on our σ_8 measurement is quite low in part because we held the values of Ω_m , h , and Γ fixed to their WMAP3 best-fit values. Allowing these values to change does alter our best fit values of c_2 and σ_8 . In order to determine the degree to which the uncertainty in these parameters should affect the uncertainty of our results, we repeated our σ_8 measurements using the $Z_{0.53}$ data set ($0.5 < z < 0.57$) and produced model $\bar{\omega}_2$ and s_3 for each parameter at the 1σ limits determined by the WMAP3 alone best-fits (while holding the other parameters at their best-fit values).

As long as the geometry of the Universe is kept flat, changes in the matter density have little effect on either the amplitude or the shape of $\bar{\omega}_2$. Thus, we expected that the value of Ω_m would have little effect on our measurement of σ_8 . This was indeed the case, as we found $\sigma_8 = 0.796 \pm 0.086$ and 0.800 ± 0.088 for Ω_m equaling 0.251 and 0.2134, respectively, with Ω_{total} fixed at 1 and $(\Gamma, h) = (0.135, 0.73)$. Conversely, we expected our measurement of σ_8 to be fairly dependent on the value of h , as this value significantly affects the distance to the LRGs. We found $\sigma_8 = 0.846 \pm 0.088$ and 0.748 ± 0.085 for $h = 0.7$ and 0.76 , respectively, with $(\Omega_{total}, \Gamma, \Omega_m) = (1, 0.135, 0.238)$. The percentage change in the measured σ_8 was approximately the same as the percentage change in h , suggesting a close relationship between the two (again, as expected).

We also expected the value of Γ to have a significant effect on the measurement, as changing Γ alters the shape of $\bar{\omega}_2$. For $\Gamma = 0.149$ and 0.12 , we found $\sigma_8 = 0.842 \pm 0.088$ and 0.736 ± 0.082 , with $(\Omega_{total}, h, \Omega_m) = (1, 0.73, 0.238)$. While the uncertainty in Γ produced the largest range in σ_8 values, the percentage change in σ_8 was actually $\sim 25\%$ smaller than the percentage change in Γ . We thus determine that although the uncertainty in Γ introduces the most uncertainty into our measurement of σ_8 , our measurement technique is most sensitive to the value of h . Despite the changes in the value of σ_8 that we measure, our measurement of σ_8 has not changed by more than 8%. This suggests that our quoted uncertainty of 0.05 would increase by less than a factor of two when uncertainties in h and Γ were taken into account. We are thus confident our measurements are accurate to within 10%.

We also assumed no error in our redshift distribution when making our measurements. Precise knowledge of the redshift distribution is necessary for Equations 3 and 7. In order to explicitly test our measurements' dependence on the redshift distribution, we created two new distributions for the $Z_{0.52}$ redshift range (see R07 for the details of how these distributions are constructed). For one, we systematically increased the error of each photometric redshift by 10% (effectively broadening the redshift distribution) and for the other we decreased the error of each photometric redshift by 10% (effectively narrowing the distribution). We then re-calculated the best-fit σ_8 for each distribution, finding that it increased to 0.84 ± 0.09 for the distribution with greater redshift errors and that it decreased to 0.76 ± 0.09 for the distribution with smaller redshift errors. These differences are significant, but are smaller than our combined 1σ error. We thus do not believe this issue significantly adds to our quoted uncertainty.

5.2. Testing via Halo Models

It is important to determine how our measured bias values compare to theoretical values. We calculate b_1 and c_2 using halo models and the methods prescribed by Nishimichi et al. (2007). They show that one can combine the N th-order bias coefficient of halos as a function of mass and redshift, $B_N(m, z)$, the number of halos of a certain mass and redshift, $n_{halo}(m, z)$, and the mean number of galaxies occupying a halo of a certain mass, $\langle n_g | M \rangle$, to find the bias of a population of galaxies. This can be expressed by

$$b_N = \frac{\int dM n_{halo}(M, z) B_N(M, z) \langle n_g | M \rangle}{\int dM n_{halo}(M, z)} \quad (9)$$

We determine both $n_{halo}(m, z)$ and $B_N(m, z)$, by using an ellipsoidal collapse model (e.g., Sheth et al. 2001) and following the methods described in detail in Nishimichi et al. (2007). For $\langle n_g | M \rangle$ we first model the number of central LRGs per halo as having a “soft” transition between $n_g = 0$ and $n_g = 1$ such that

$$\langle n_{central} | M \rangle = 0.5 \left[1 + \text{erf} \left(\frac{\log_{10}(M/M_{cut})}{\sigma_{cut}} \right) \right] \quad (10)$$

as in Zheng et al. (2005) and Blake et al. (2007a). This helps account for the fact that we are not using a volume-limited sample, and thus at smaller redshifts the mass limit is likely to be smaller than at higher redshifts. As in Blake et al. (2007a), we model the number of satellite galaxies using a simple power law. Thus

$$\langle n_{sat} | M \rangle = \left(\frac{M}{M_0} \right)^\alpha \quad (11)$$

The bias model has four free parameters, M_{cut} , M_0 , σ_{cut} , and α . It is beyond the scope of this paper to fit for these parameters. It is instead our intention to determine if reasonable values for these parameters can reproduce the bias values that we measure. If this is possible, it suggests that the our bias measurements are themselves reasonable. Using $\sigma_8 = 0.793$, $z = 0.532$ and halo parameters $\log_{10}(M_{cut}/M_\odot) = 13.3$, $\sigma_{cut} = 0.6$, $\log_{10}(M_0/M_\odot) = 14.5$, and $\alpha = 2.0$, we find $b_1 = 1.61$ and $c_2 = 0.09$ — results that are consistent with our best-fit values. The values of $\log_{10}(M_0/M_\odot)$ and σ_{cut} were chosen to be equal to the best-fit parameters found by Blake et al. (2007a) for LRGs with $0.5 < z < 0.55$. The $\log_{10}(M_{cut}/M_\odot)$ and α parameters are slightly lower than the Blake et al. (2007a) parameters likely because our LRGs have a lower luminosity and thus a lower bias, minimum mass, and α (α has been seen to increase with b_1 in both Blake et al. 2007a and Zehavi et al. 2005). This is not to suggest that we favor a steep power-law to a shallow one. If we change $\alpha = 1.4$ (as measured by Kulkarni et al. 2007), we calculate $b_1 = 1.62$ and $c_2 = 0.09$ if we also

reduce $\log_{10}(M_0/M_\odot)$ to 14.41. This implies that, from a theoretical standpoint and in the context of relevant measurements of LRG halo properties, our measurements of b_1 and c_2 are reasonable.

The bias model can also be used to test our implicit assumption that $\langle c_2 \rangle = \langle b_2 \rangle / \langle b_1 \rangle$. We calculate b_1 , b_2 , and c_2 at redshifts between 0.4 and 0.7 (essentially the redshift range of our entire sample) in intervals of 0.02. These values are used to calculate theoretical values for $\langle b_2 \rangle / \langle b_1 \rangle$ and $\langle b_2 / b_1 \rangle$. We find that the difference between the two is less than 0.1%, meaning that the systematic error introduced by assuming $\langle c_2 \rangle = \langle b_2 \rangle / \langle b_1 \rangle$ is insignificant for our measurements.

5.3. Comparison With Other Measurements

Our measurement of $\sigma_8 = 0.789 \pm 0.050$ is consistent with most previous measurements. There are, however, notable exceptions. Our result is inconsistent to 1σ with a photometric optical cluster counting technique employing SDSS data that found $\sigma_8 = 0.92 \pm 0.10$ (Rozo et al. 2007). Another recent result (Harker et al. 2007) found a similarly high value of $\sigma_8 = 0.97 \pm 0.06$ using N-body simulations in combination with semi-analytic galaxy formation models and the projected two-point correlation function of SDSS galaxies. Other results determine σ_8 to be too small to be consistent with our measurement (to 1σ). Notable examples are the WMAP3 constrained by inflationary models result of 0.702 ± 0.062 (Spergel et al. 2007) and the Voevodkin & Vikhlinin (2004) results that found $\sigma_8 = 0.72 \pm 0.04$ by using the cluster baryon mass function.

However, many notable results are consistent with our measurement. The best fit WMAP3 data alone found $\sigma_8 = 0.744^{+0.05}_{-0.06}$, which is just barely consistent with our measurement to 1σ . The WMAP3+SDSS and WMAP3+LRG best-fit values of $\sigma_8 = 0.772^{+0.036}_{-0.048}$ and $0.781^{+0.032}_{-0.045}$ are consistent with our measurement to less than 1σ . Large disagreement with these results would be surprising, given that we used WMAP3 best-fit priors for the relevant input cosmological parameters. The WMAP5 results are quite similar to our results, as Komatsu et al. (2008) find $\sigma_8 = 0.796 \pm 0.036$, for the WMAP alone five-year mean value. More significantly, our results are also consistent to 1σ with $\sigma_8 = 0.67^{+0.18}_{-0.13}$ as derived from optical cluster finding techniques (Gladders et al. 2007) and $\sigma_8 = 0.66 \pm 0.16$ from x-ray cluster measurements (Henry 2004). Due to the fact that the inconsistent measurements appear to be as likely to be lower than our measurement as they are higher, we feel that these results are hinting at a potential convergence to a σ_8 value that is close to 0.8.

6. Conclusions

We present and test a new method for determining the value of σ_8 . The method and the results of our testing can be summarized as follows:

- The technique for measuring σ_8 utilizes two measures of the second-order bias of a density field. The two methods have different dependencies on the value of σ_8 , and can thus be combined to determine a best-fit σ_8 and second-order bias. One measure of the second-order bias (the *R07* method) has been used many times before (e.g., R07) and depends on the amplitude of s_3 . The other method (the *shape* method) has (to our knowledge) never been used before. It relies on correcting the overdensities for given first- and second-order bias parameters and determining the bias parameters that allow the shapes of the $\bar{\omega}_2$ measurement and model to become consistent.

- The method was tested using a mock catalog of LRGs drawn from the Blaizot all-sky catalog (Blaizot et al. 2005) that was constructed using Millennium Simulation data (Springel et al. 2005) and its input cosmological parameters for Ω_m , h , and Γ . The Millennium Simulation assumed $\sigma_8 = 0.9$ and we measured $\sigma_8 = 0.898 \pm 0.062$. This measurement proved that our method is both accurate and precise.

- We photometrically selected LRGs from SDSS DR5, determined photometric redshifts for each LRG, and removed stars following the prescriptions of Collister et al. (2007). We divided this LRG catalog into three samples by redshift, with the separate ranges being $0.4 < z < 0.5$ ($Z_{0.47}$), $0.5 < z < 0.57$ ($Z_{0.53}$), and $0.57 < z < 0.7$ ($Z_{0.61}$).

- We measured σ_8 in each sample and found $\sigma_8 = 0.776 \pm 0.080$, $\sigma_8 = 0.796 \pm 0.086$, and $\sigma_8 = 0.798 \pm 0.094$, respectively. Combining these consistent results we determined $\sigma_8 = 0.789 \pm 0.050$. For each measurement, we assumed the relevant cosmological parameters were equal to their WMAP3 best-fit values.

- Allowing the relevant cosmological parameters to vary within their WMAP3 1σ error, we found our measurement of σ_8 changed by less than 8%. Thus, even allowing for these uncertainties, our method produces a precise measurement that we are confident is accurate to within 10%.

- We measured $b_{1,Z_{0.47}} = 1.47 \pm 0.09$, $b_{1,Z_{0.53}} = 1.65 \pm 0.09$, and $b_{1,Z_{0.61}} = 1.80 \pm 0.10$ and $c_{2,Z_{0.47}} = 0.09 \pm 0.04$, $c_{2,Z_{0.53}} = 0.09 \pm 0.05$, and $c_{2,Z_{0.61}} = 0.09 \pm 0.03$. Using a halo model, we determined that the bias values for $Z_{0.53}$ were consistent with reasonable, and previously measured, HOD parameters.

The techniques described herein can easily be repeated and tested using other cosmic samples. Future surveys, such as the Panoramic Survey Telescope & Rapid Response System

(Pan-STARRS), the Dark Energy Survey (DES), and the Large Synoptic Survey Telescope (LSST), will provide opportunities to measure both the 2- and 3-point area averaged correlation functions to extreme precision. Repeating the techniques we have presented here will allow researchers to determine σ_8 accurately, precisely, and independently of future cluster counting and CMB techniques, thus providing an important check on those results.

In addition to our determinations of the bias and of σ_8 , we have found that a feature in the hierarchical amplitude of s_3 at $\sim 10 h^{-1}\text{Mpc}$ exists in two of the three data sets. Given that a feature existed at approximately the same physical location for early-type galaxies at significantly smaller redshifts (R07), the feature appears physical in nature. The fact that it is absent in one of our data sets hints that the possible cause may be due to projection effects, or that perhaps the feature is indicative of complicated halo occupation statistics. The feature demands further study, both observationally and theoretically, and we are currently focusing our efforts to explain this phenomenon.

AJR, RJB and ADM acknowledge support from Microsoft Research, the University of Illinois, and NASA through grant NNG06GH156. The authors made extensive use of the storage and computing facilities at the National Center for Supercomputing Applications and thank the technical staff for their assistance in enabling this work.

We thank Anil Thakur and Jan Van den Berg for help with obtaining a copy of the SDSS DR5 databases. We thank Ravi Sheth for comments that helped improve the paper. We thank an anonymous referee whose comments helped us to significantly improve our results.

Funding for the creation and distribution of the SDSS Archive has been provided by the Alfred P. Sloan Foundation, the Participating Institutions, the National Aeronautics and Space Administration, the National Science Foundation, the U.S. Department of Energy, the Japanese Monbukagakusho, and the Max Planck Society. The SDSS Web site is <http://www.sdss.org/>.

The SDSS is managed by the Astrophysical Research Consortium (ARC) for the Participating Institutions. The Participating Institutions are The University of Chicago, Fermilab, the Institute for Advanced Study, the Japan Participation Group, The Johns Hopkins University, the Korean Scientist Group, Los Alamos National Laboratory, the Max-Planck-Institute for Astronomy (MPIA), the Max-Planck-Institute for Astrophysics (MPA), New Mexico State University, University of Pittsburgh, University of Portsmouth, Princeton University, the United States Naval Observatory, and the University of Washington.

REFERENCES

- Bernardeau, F. 1995, *A&A*, 301, 309
- Bernardeau, F., Colombi, S., Gaztañaga, E., & Scoccimarro, R. 2002, *Phys. Rep.*, 367, 1
- Blaizot, J., Wadadekar, Y., Guiderdoni, B., Colombi, S. T., Bertin, E., Bouchet, F. R., Devriendt, J. E. G., & Hatton, S. 2005, *MNRAS*, 360, 159
- Blake, C., Collister, A., Bridle, S., & Lahav, O. 2007, *MNRAS*, 374, 1527
- Blake, C., Collister, A., & Lahav, O. 2007, *ArXiv e-prints*, 704, arXiv:0704.3377
- Cannon, R., et al. 2006, *MNRAS*, 372, 425
- Cole, S., et al. 2005, *MNRAS*, 362, 505
- Collister, A., et al. 2007, *MNRAS*, 375, 68
- Davis, M., & Peebles, P. J. E. 1983, *ApJ*, 267, 465
- Eisenstein, D. J., & Hu, W. 1998, *ApJ*, 496, 605
- Firth, A. E., Lahav, O., & Somerville, R. S. 2003, *MNRAS*, 339, 1195
- Fry, J. N., & Gaztanaga, E. 1993, *ApJ*, 413, 447
- Gaztanaga, E. 1992, *ApJ*, 398, L17
- Gladders, M. D., Yee, H. K. C., Majumdar, S., Barrientos, L. F., Hoekstra, H., Hall, P. B., & Infante, L. 2007, *ApJ*, 655, 128
- Harker, G., Cole, S., & Jenkins, A. 2007, *MNRAS*, 382, 1503
- Henry, J. P. 2004, *ApJ*, 609, 603
- Kaiser, N. 1984, *ApJ*, 284, L9
- Koester, B. P., et al. 2007, *ApJ*, 660, 221
- Komatsu, E., et al. 2008, *ArXiv e-prints*, 803, arXiv:0803.0547
- Kulkarni, G. V., Nichol, R. C., Sheth, R. K., Seo, H.-J., Eisenstein, D. J., & Gray, A. 2007, *MNRAS*, 378, 1196
- Limber, D. N. 1954, *ApJ*, 119, 655

- Myers, A. D., Outram, P. J., Shanks, T., Boyle, B. J., Croom, S. M., Loaring, N. S., Miller, L., & Smith, R. J. 2003, MNRAS, 342, 467
- Myers, A. D., Outram, P. J., Shanks, T., Boyle, B. J., Croom, S. M., Loaring, N. S., Miller, L., & Smith, R. J. 2005, MNRAS, 359, 741
- Myers, A. D., et al. 2006, ApJ, 638, 622
- Myers, A. D., et al. 2007, ApJ, 658, 85
- Nishimichi, T., Kayo, I., Hikage, C., Yahata, K., Taruya, A., Jing, Y. P., Sheth, R. K., & Suto, Y. 2007, PASJ, 59, 93
- Padmanabhan, N., et al. 2007, MNRAS, 378, 852
- Peebles, P. J. E. 1980, Research supported by the National Science Foundation. Princeton, N.J., Princeton University Press, 1980. 435 p.
- Pierpaoli, E., Borgani, S., Scott, D., & White, M. 2003, MNRAS, 342, 163
- Riess, A. G., et al. 2004, ApJ, 607, 665
- Ross, A. J., Brunner, R. J., & Myers, A. D. 2006, ApJ, 649, 48
- Ross, A. J., Brunner, R. J., & Myers, A. D. 2007, ApJ, 665, 67
- Rozo, E., et al. 2007, ArXiv Astrophysics e-prints, arXiv:astro-ph/0703571
- Sheth, R. K., Mo, H. J., & Tormen, G. 2001, MNRAS, 323, 1
- Simon, P. 2007, A&A, 473, 711
- Smith, R. E., et al. 2003, MNRAS, 341, 1311
- Scranton, R., et al. 2002, ApJ, 579, 48
- Spergel, D. N., et al. 2003, ApJS, 148, 175
- Spergel, D. N., et al. 2007, ApJS, 170, 377
- Springel, V., et al. 2005, Nature, 435, 629
- Tegmark, M., et al. 2004, Phys. Rev. D, 69, 103501
- Voevodkin, A., & Vikhlinin, A. 2004, ApJ, 601, 610

Zehavi, I., et al. 2005, ApJ, 621, 22

Zheng, Z., et al. 2005, ApJ, 633, 791

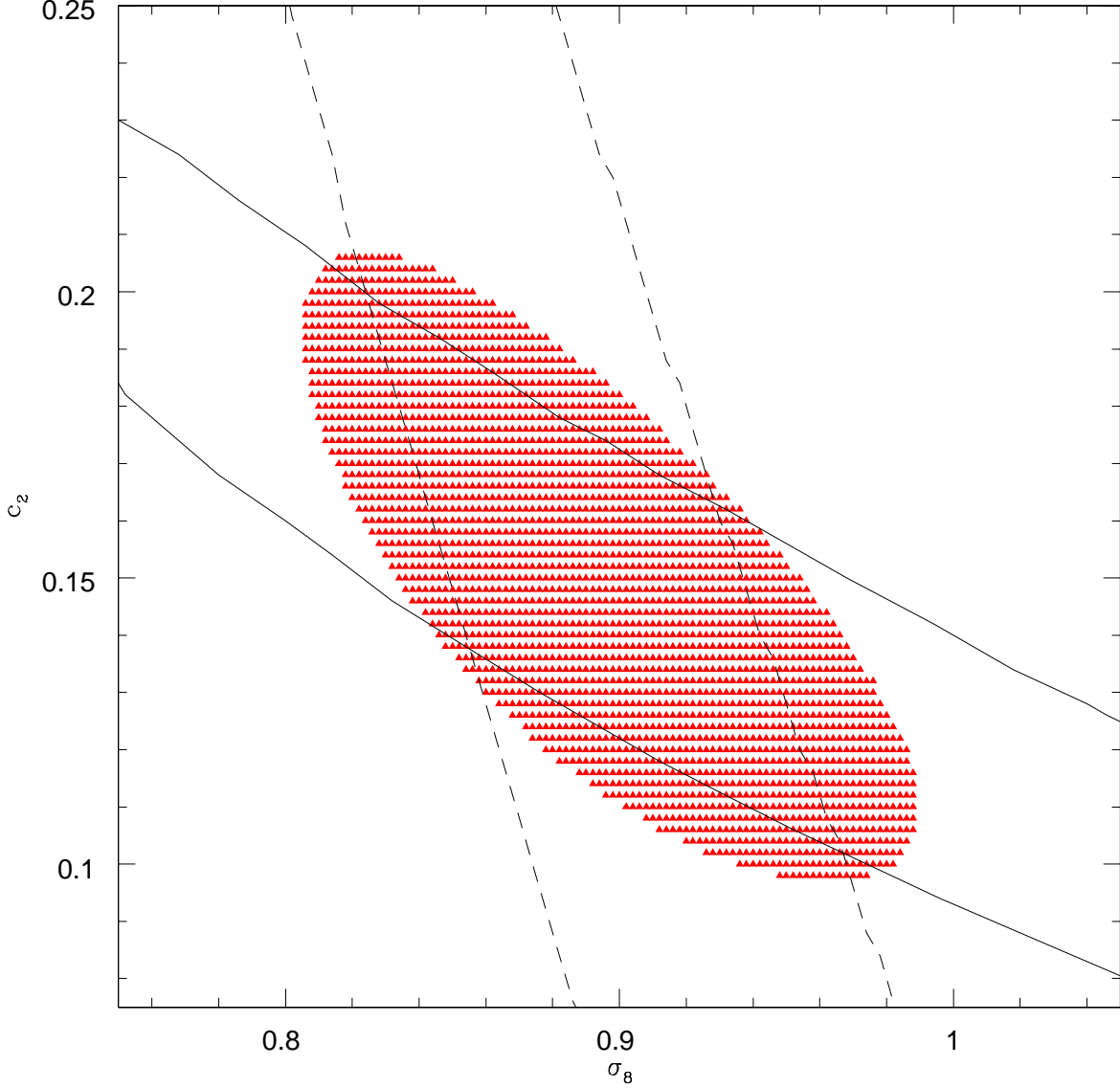


Fig. 1.— The 1σ allowed regions for c_2/σ_8 determined by the shape method (solid black lines) and the R07 method (dashed black lines) for simulated LRGs from the Blaizot all-sky mock catalog (Blaizot et al. 2005) created using Millennium simulation data (Springel et al. 2005). These measurements are combined to produce the 1σ (red) allowed region. The 1σ best-fit values are $c_2 = 0.15 \pm 0.04$ and $\sigma_8 = 0.898 \pm 0.062$, consistent with the Millennium input value of $\sigma_8 = 0.9$

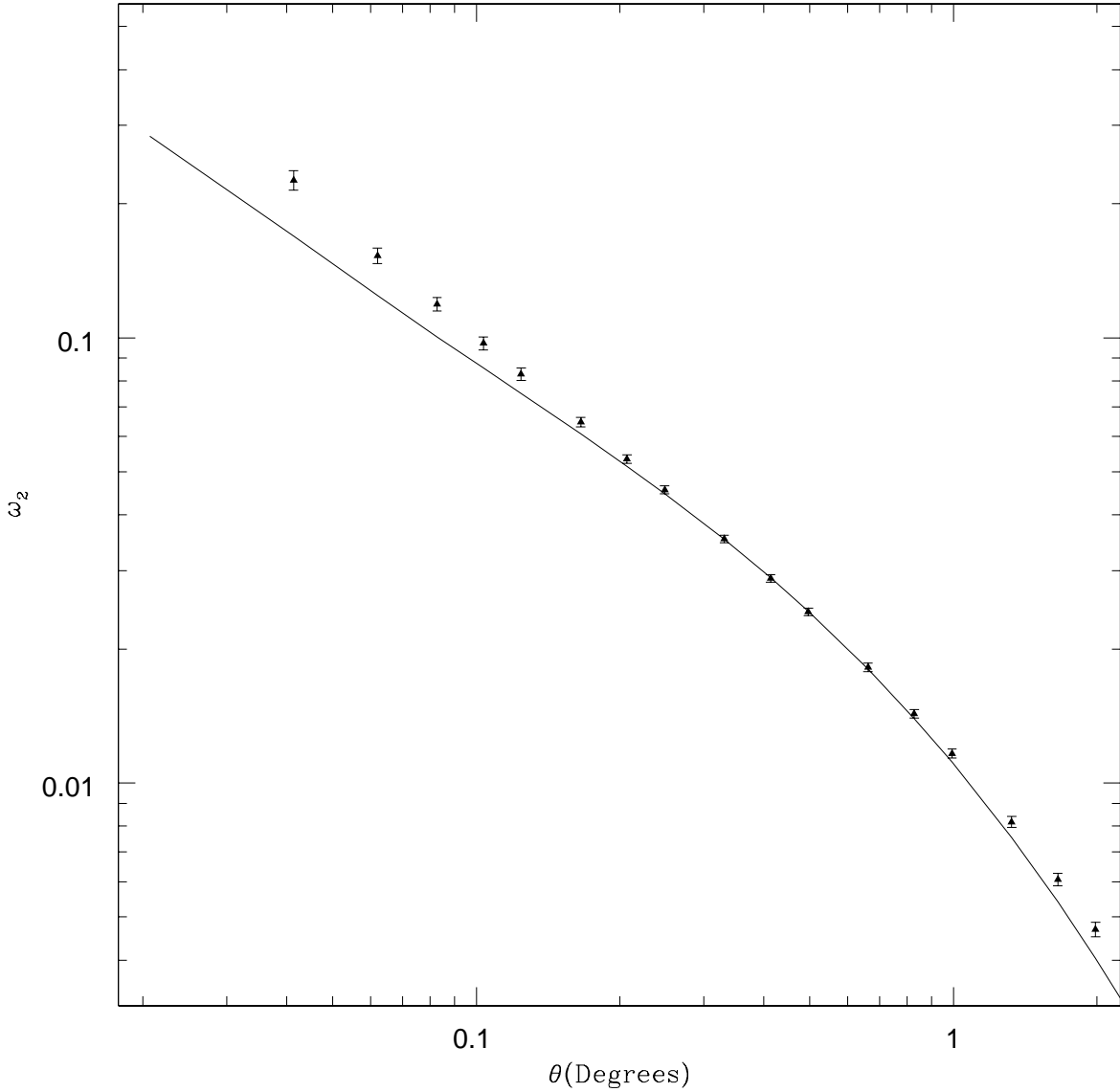


Fig. 2.— The area-averaged angular two-point correlation function for photometrically-classified LRGs from SDSS DR5 with photometric redshifts $0.5 < z < 0.57$ ($Z_{0.53}$), divided by 1.63^2 (black triangles, $b_1 = 1.63$ for $\sigma_8 = 0.8$). The solid line represents the model $\bar{\omega}_2$ calculated using Smith et al. (2003) power spectra and Limber’s equation. At scales smaller than 0.25° , the measurement is larger than the model, suggesting positive second order bias.

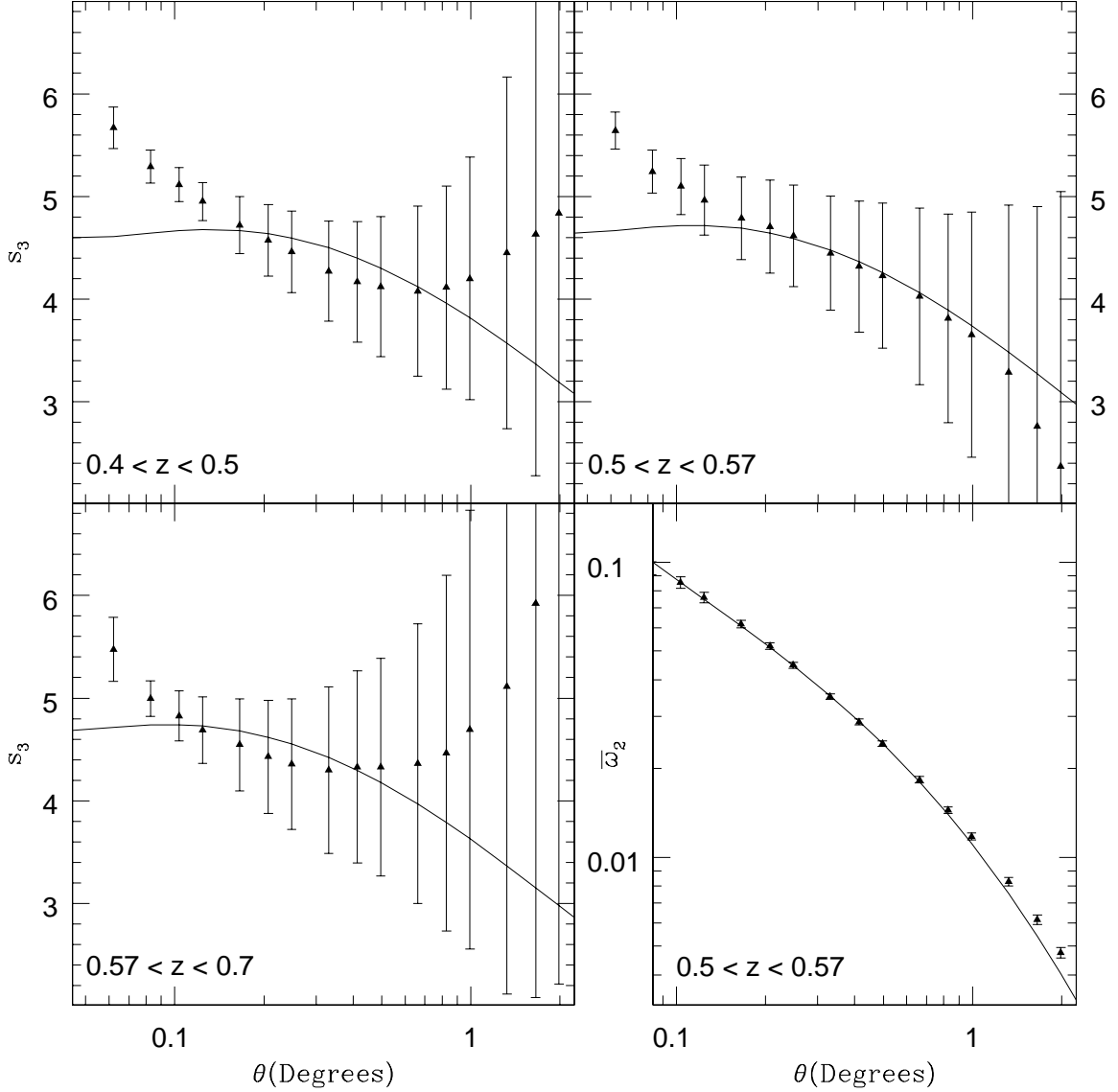


Fig. 3.— Left to right, top to bottom, the first three panels display the measured s_3 (black triangles) for photometrically classified LRGs from SDSS DR5 with photometric redshifts $0.4 < z < 0.5$ ($Z_{0.47}$), $0.5 < z < 0.57$ ($Z_{0.53}$), and $0.57 < z < 0.7$ ($Z_{0.61}$). In order to take the bias into account, s_3 is divided by the best-fit b_1 and then has three times the best-fit c_2 subtracted from it for each respective redshift range (for $\sigma_8 = 0.8$). The solid line in each of these three panels is the model s_3 for $\sigma_8 = 0.8$. The $Z_{0.53}$ data has a different shape than the other data sets at large scales, but due to the size of the error bars, all data sets are consistent with the model s_3 to at least 96%. The lower-right panel displays the bias-corrected measurement of \bar{w}_2 (black triangles) for $Z_{0.53}$ using the best-fit $b_1 = 1.63$, and $b_2 = 0.15$ for $\sigma_8 = 0.8$. The solid black line is the model \bar{w}_2 for $\sigma_8 = 0.8$. Visually, the fit appears to be as good as the $\chi^2 = 0.6$, $P(< \chi^2) = 0.998$ suggests.

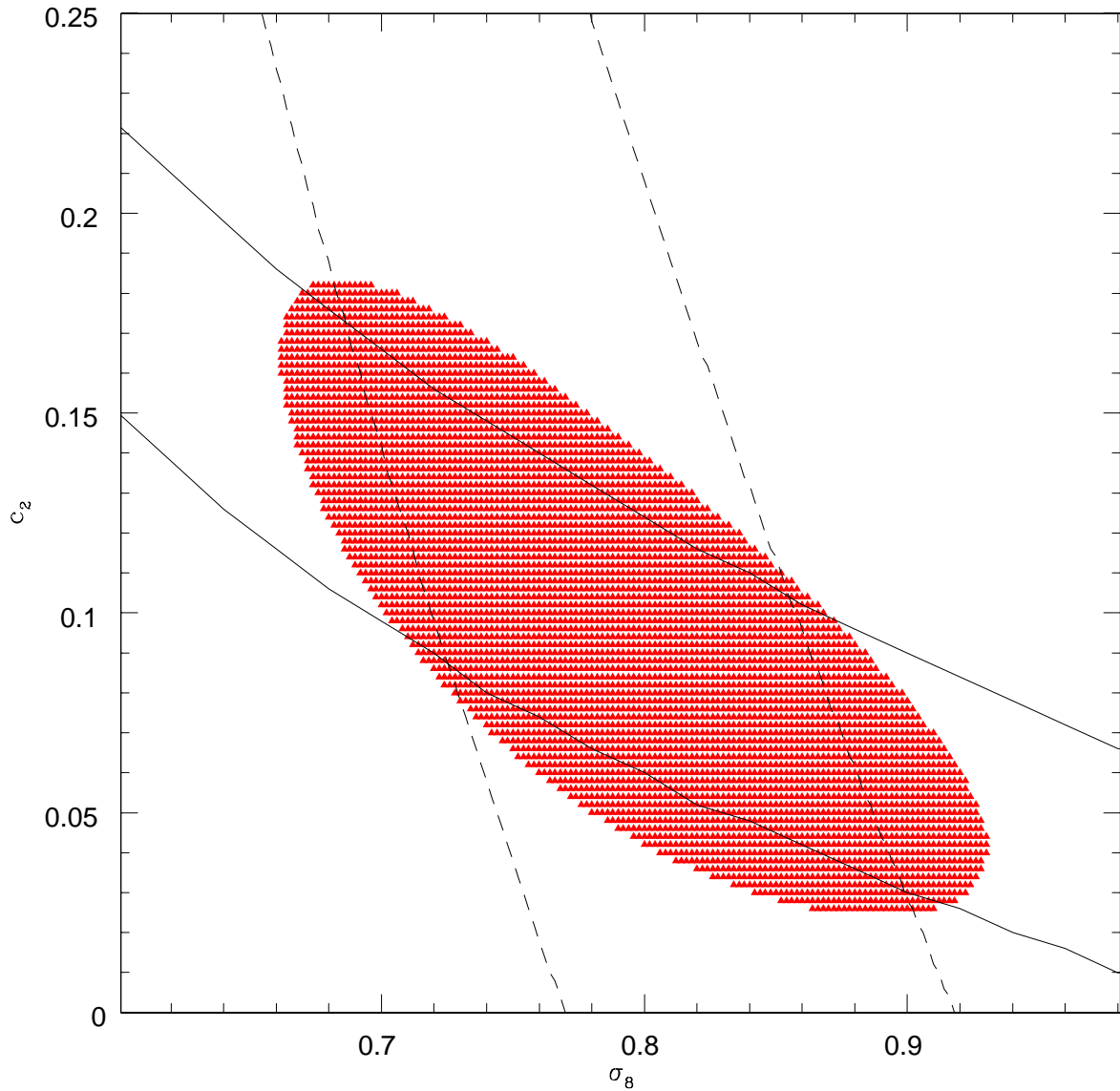


Fig. 4.— The 1σ allowed regions for c_2/σ_8 determined by the *R07* method (dashed black lines) and the *shape* method (solid black lines) for photometrically selected LRGs from SDSS DR5 with $0.5 < z < 0.57$ ($Z_{0.53}$). These measurements are combined to produce the 1σ (red) allowed region. The 1σ best-fit values are $c_2 = 0.092 \pm 0.052$ and $\sigma_8 = 0.796 \pm 0.086$.